THE ASTROPHYSICAL JOURNAL, 309:275–293, 1986 October 1

ROTATIONAL AND RADIAL VELOCITIES OF T TAURI STARS[1]

L. HARTMANN, R. HEWETT, S. STAHLER, AND R. D. MATHIEU
Harvard-Smithsonian Center for Astrophysics
Received 1985 December 26; accepted 1986 March 21

ABSTRACT

We report rotational and radial velocities for 50 T Tauri stars in the Taurus-Auriga and Orion complexes. Our results provide the first measurements of rotation for many low-mass pre–main-sequence stars and show that the radial velocity dispersion of T Tauri stars relative to associated molecular cloud gas is $\lesssim 1.5$ km s^{-1}. We confirm and extend the finding of Vogel and Kuhi that most T Tauri stars are slow rotators, with rotation and order of magnitude or more below breakup velocity. About 30% of the 0.5–1.0 $M_\odot$ stars in Taurus-Auriga have rotational velocities at or below our detection limit of 10 km s^{-1}; half have $v \sin i$ values between 10 and 15 km s^{-1}. T Tauri stars in the mass range 0.7–1.5 $M_\odot$ have angular momenta per unit mass between 30 and 200 times the present solar value; most of these stars have less angular momentum than is at present in the solar system.

Our observed low rotation rates show that low-mass stars have lost most of the angular momentum of their parent interstellar clouds by the time they first appear optically. This substantial loss must occur either during protostellar collapse or within $\sim 10^5$ yr after its cessation. The distribution of $v \sin i$ is inconsistent with the hypothesis that all stars of the same mass and age have the same rotational velocity and a random orientation of rotation axes. The results show instead a significant spread in angular momentum among these stars, indicating a corresponding dispersion in initial conditions.

Comparison with rapidly rotating main-sequence stars in the young α Per cluster indicates that T Tauri stars in the mass range 0.5–1.0 $M_\odot$ lose at most about three-quarters of their angular momentum as they spin-up during pre–main-sequence contraction. This limit on angular momentum loss is consistent with wind models for these stars.

The new rotational velocity measurements allow us to investigate the emission-rotation relation for low-mass T Tauri stars for the first time. We find no correlation between Hα emission and rotation among low-mass T Tauri stars, suggesting that T Tauri activity may not be driven by a solar-type magnetic dynamo.

Subject headings: radial velocities — stars: pre-main sequence — stars: rotation

I. INTRODUCTION

One of the major gaps in our understanding of stellar physics is the role of angular momentum in the formation and early life of a star. Two problems of great interest are the transport of angular momentum in collapsing interstellar clouds and the subsequent braking of young stars during pre–main-sequence contraction. The evolution of stellar rotation may also play an important role in the powerful emission activity characteristic of young stars, if an activity-rotation connection similar to that of main-sequence stars is present. Accurate rotational velocity measurements of young stars are essential for further progress in these areas.

The first systematic investigation in this area was conducted by Vogel and Kuhi (1981), who observed 64 pre–main-sequence stars in NGC 2264 and in the Taurus-Auriga region. The vast majority of stars in their sample are slow rotators, in the sense that the observed surface velocities fall well below breakup speeds. Indeed, three-quarters of their sample had rotation speeds below their detection limits of 25–35 km s^{-1}; for all but one star with $M < 1.25\ M_\odot$, only upper limits on $v \sin i$ could be obtained. Clearly, a better determination of this fundamental stellar parameter is of considerable astrophysical interest.

In this paper we provide rotational velocities of 50 T Tauri stars in the Taurus-Auriga and Orion complexes. Twenty-five of the 33 stars with $M < 1\ M_\odot$ in our sample have rotational velocities above our detection limit of 10 km s^{-1}. Many of these stars have positions in the H-R diagram which make them among the youngest optically visible stars in their associations. Thus, our data provide important observational constraints on theories of angular momentum loss during both protostellar collapse and early pre–main-sequence evolution.

The 0.5–1.0 $M_\odot$ stars in our sample have angular momenta $\sim$20–100 times the present solar value. By combining our observations with data from the young galactic open cluster α Per, we find that stars in the mass range 0.5–1.0 $M_\odot$ lose at most about three-fourths of their T Tauri angular momentum by a contraction age of 5×10^7 yr. This limitation on angular momentum loss during the T Tauri phase is consistent with current wind models for these stars. Our data suggest that the distribution of rotational velocities for T Tauri stars with a common mass and radius is skewed toward low velocities. Interestingly, a qualitatively similar distribution of rotation is also seen in young open clusters.

It has been suggested that T Tauri stars have extensive, dense, solar-type chromospheres which are responsible for much of the optical line emission observed (Herbig 1970; Cram 1979; Herbig and Soderblom 1980; Calvet, Basri, and Kuhi 1984). Because chromospheric and coronal emission is strongly dependent upon rotation for late-type main-sequence stars (Kraft 1967; Skumanich 1972; Pallavicini *et al.* 1981; Walter

[1] Research reported herein used the Multiple Mirror Telescope, a joint facility of the Smithsonian Institution and the University of Arizona.

1982; Noyes *et al.* 1984; Hartmann *et al.* 1984), a similar correlation may be observable in T Tauri stars. As a first step in this direction, we have searched for, but not found, a significant correlation between Hα emission and rotation in our sample.

We also report radial velocities for our program objects. Most stars have velocities within $\lesssim 1.5$ km s^{-1} of the velocities of the associated molecular cloud material, emphasizing the close association found by Herbig (1977*a*) of T Tauri stars with their parent material. There is evidence that some of our stars are spectroscopic binaries; we defer discussion of these data to a later paper.

In § II we describe the nature of the spectroscopic data and the methods we used to derive values of $v \sin i$. In § III we present results and comment on individual objects of interest. In § IV the observed rotational velocity distributions are analyzed, and in § V we consider the implications of our results for star formation, stellar spin-down, and emission-line activity.

II. OBSERVATIONS

a) High-Resolution Spectra

We have obtained high-resolution observations using the echelle spectrographs and intensified Reticon detectors on the MMT and the 1.5 m telescope of the Fred L. Whipple Observatory on Mount Hopkins. Details of the instrumentation are given by Latham (1982). Our observations were restricted to a 44 Å bandpass centered near 5200 Å. The spectral resolution of the data is ~ 12 km s^{-1}. Similar data were analyzed to obtain rotational velocities for late-type stars in the Pleiades and α Per clusters (Stauffer *et al.* 1984, 1985).

Typical T Tauri spectra are shown in Figure 1. Most stars exhibit a fairly normal late-type spectrum, while the photospheric lines of other objects are completely obscured by emission lines and continuua. The λ5183 line of Mg I is observed in emission for some of the most active emission-line stars. Detailed comments on individual spectra of particular interest are deferred to a later section.

b) Rotation Analysis

We chose to measure rotational velocities using cross-correlation analysis (see Tonry and Davis 1979; Latham 1985). The cross-correlation is normally accomplished by multiplying the discrete Fourier transforms of object and template spectra together, and then inverse-transforming the result. The correlation peak is then fitted using an artificially broadened template star to measure the $v \sin i$. We previously reported results using the cross-correlation technique for stars in the Pleiades and α Per clusters (Stauffer *et al.* 1984, 1985). Here we shall give a precise description of our present methodology.

We begin the velocity analysis by rebinning the echelle spectra into constant logarithmic wavelength intervals. A quadratic fit to the spectrum is then subtracted from the data

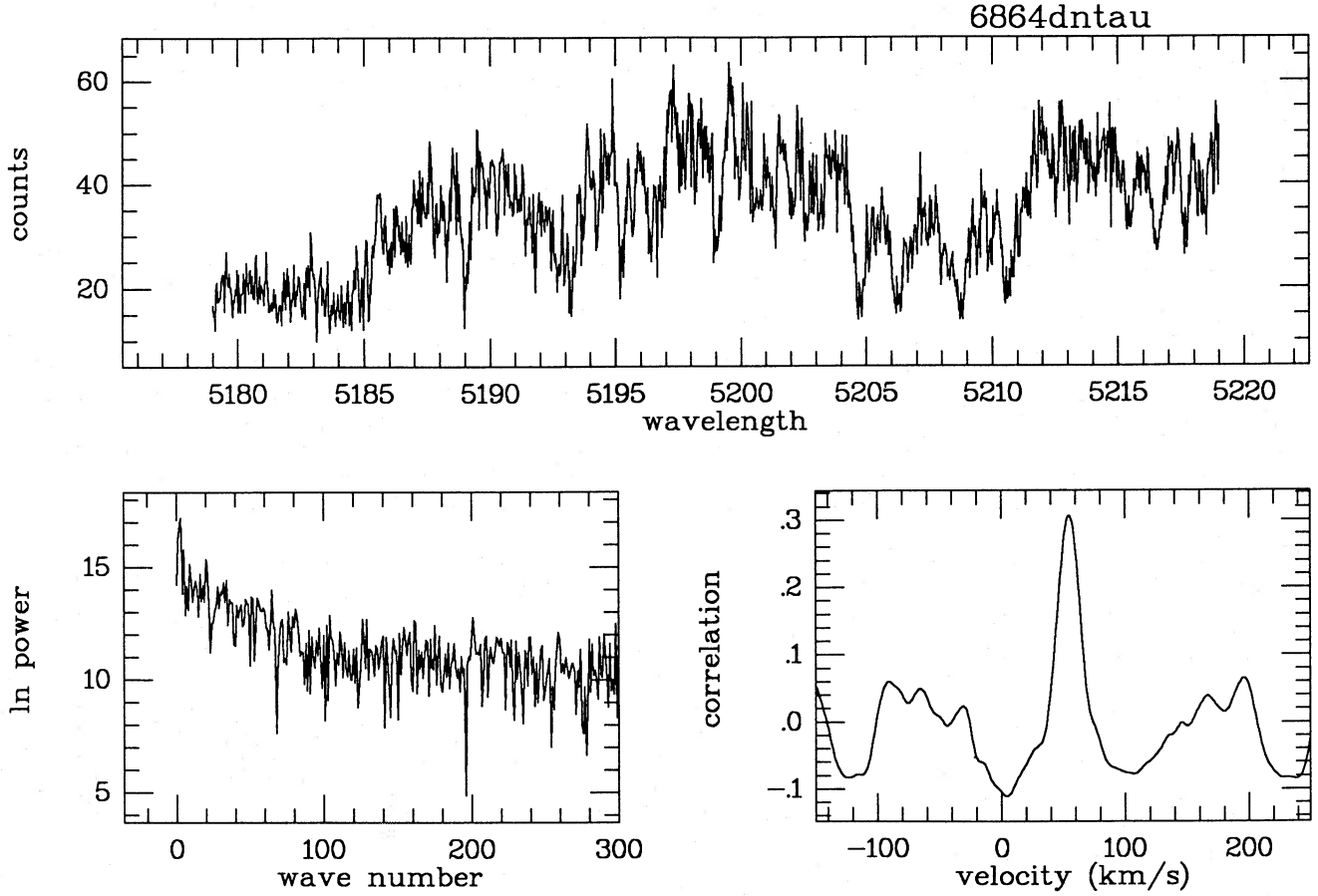

FIG. 1*a*

FIG. 1.—Wavelength-calibrated spectra, power spectra, and cross-correlations with a template K5 dwarf star for two representative T Tauri stars (see text). (*a*) DN Tau, $v \sin i \leq 10$ km s^{-1}. (*b*) RY Tau, $v \sin i = 49$ km s^{-1}.

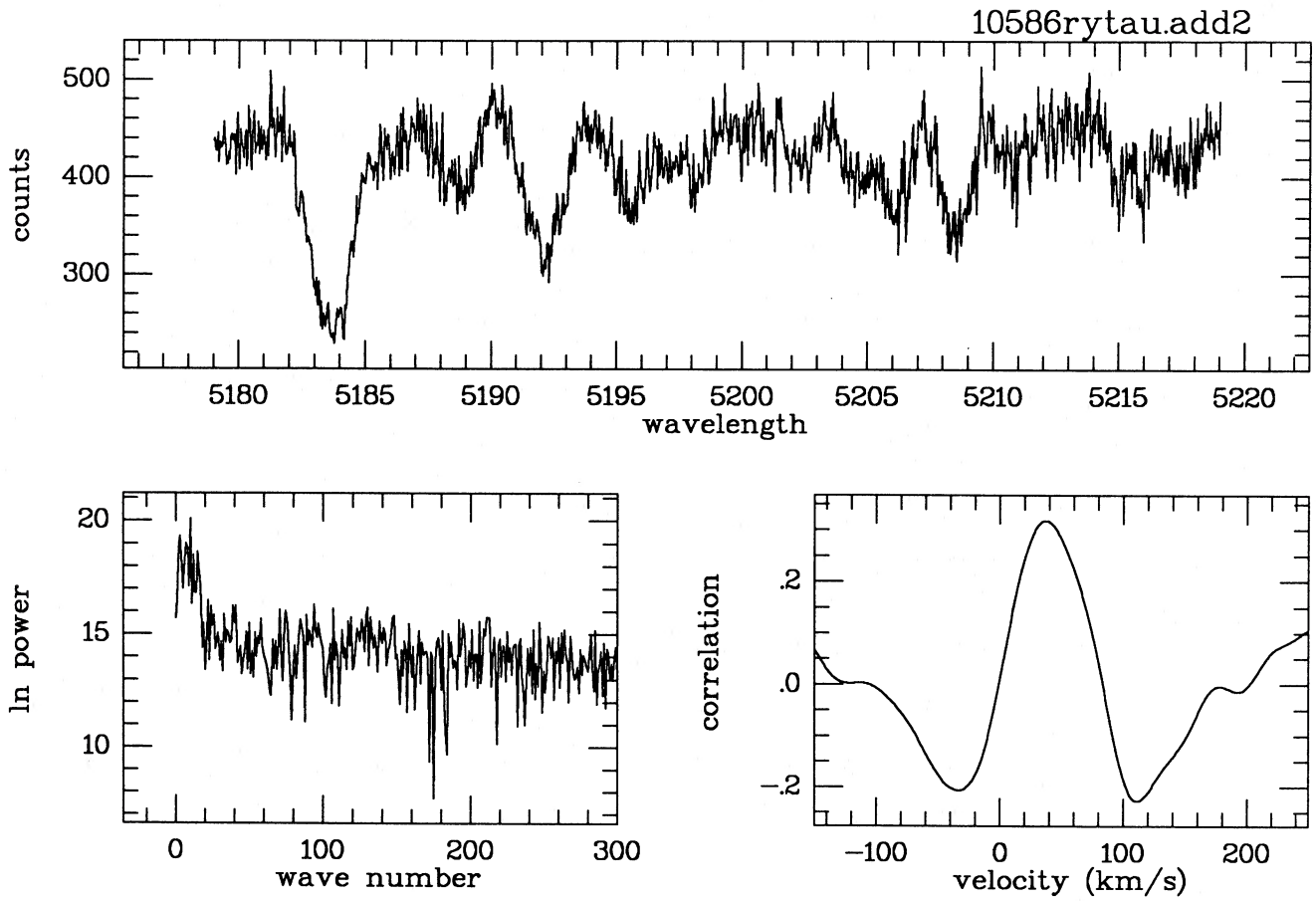

FIG. 1*b*

in order to remove trends from the data. The resulting spectrum is then endmasked using a cosine bell over 10% at each end of the spectrum (see Brault and White 1971). The spectrum is Fourier transformed, and multiplied by a similarly prepared transform of a template spectrum. This product is filtered in a manner described in more detail below, and the result is inverse-transformed, producing the cross-correlation.

Our original spectra consist of 2048 pixels, with ~ 45 Å of useful spectrum displayed over ~ 1500 pixels. Thorium-argon comparison spectra are used to establish the pixel-to-wavelength conversion, with an rms error ~ 0.012 Å. About 10% of the spectrum is unusable because the wavelength fit does not extend accurately to the ends. For convenience in Fourier transformation, the data are expanded by linear interpolation into 2048 logarithmic wavelength bins corresponding to ~ 1.2 km s^{-1} per bin from the original ~ 1.6 km s^{-1} per bin. With our instrumental resolution of ~ 12 km s^{-1}, there is little information at wavenumbers $\gtrsim 150$ (see Fig. 1). Conservatively, our standard filter uses a cosine bell to taper off the transform to zero between wavenumbers 200 and 300. The low-frequency end of our standard filter is another cosine bell, running between wavenumbers 5 and 20. This has the result of removing most of the effect of the $\lambda 5183$ line of Mg I, which is strongly opacity broadened, on the width of the correlation peak (see Fig. 1).

For a rapidly rotating star like RY Tau (Fig. 1*b*), different filtering is appropriate. The first zero of the transform of the rotational broadening function for rotation at 40 km s^{-1} occurs at a wavenumber of ~ 40. Since there is little information in our spectra of rapid rotators beyond this wavenumber, the high-frequency cutoff of our filter begins at wavenumber 40 and drops to zero at wavenumber 60. We also retain more low frequencies for rapid rotators; the low-frequency end of the rapid rotator filter rises to unity at wavenumber 10 from a value of zero at wavenumber 3. We removed the Mg I $\lambda 5183$ from the spectra of rapid rotators by truncating the wavelength region being considered. If we had not done so, this strongly opacity-broadened line could have produced spuriously wide cross-correlation peaks using the low-frequency filter.

The correlation peak is the convolution of the stellar and instrumental profiles with the rotational broadening function. For simplicity we fitted the peak with a parabola (see Tonry and Davis 1979; Tonry 1981). The center of the parabola defines the radial velocity of the object, while the width of the parabola is calibrated by fitting the peaks of a cross-correlation between the template and another star whose spectrum has been synthetically broadened by rotation. We generated this calibration by convolving the spectrum of a standard K5 dwarf star with the rotational broadening function, assuming a standard limb-darkening law with a limb-darkening coefficient of 0.6 (see Gray 1976). These synthetically broadened spectra were convolved with the same template used for analyzing the program stars, and the parabolic width was measured for each value of $v \sin i$. (Our spectra are not of

sufficient quality to demonstrate unambiguously that the broadening is due to rotation; we simply assume that broadening > 10 km s^{-1} in these stars is due to rotation.)

The velocity interval over which the correlation peak is fitted should be restricted for best results. Using too small an interval reduces the signal-to-noise of the derived rotational and radial velocities; intervals that are too large also include unwanted correlations of different spectral features against each other, as well as extra noise. Tests of repeat spectra of selected objects and of spectra with randomly generated artificial noise added showed that we could accomplish this limitation of velocity interval simply by fitting the correlation peak to a specified level. On the basis of these tests, we adopted fits down to 50% of the correlation peak height for all stars with $v \sin i < 20$ km s^{-1}. This prescription could not be followed for rapidly rotating stars; the algorithm resulted in a tendency to fit small noise peaks superposed on the much broader correlation peak. We found that fitting down to the zero level of the correlation peak worked well for stars rotating more rapidly than 20 km s^{-1}. Our tests with repeat spectra and with noise-added spectra show that there is no systematic difference in using the half-level or zero-level fits for $v \sin i$ in the range 17–25 km s^{-1}, so that we are justified in switching at 20 km s^{-1}. We have experimented with more complicated iterative schemes, but given the relatively modest signal to noise of our spectra and the likely size of systematic errors, the above method is found to be simple and reliable.

A useful measure of signal to noise of the correlation is R, the ratio of the correlation peak height to the rms antisymmetric component R (see Tonry and Davis 1979). Tonry and Davis (1979) suggest that the errors in the radial velocity and the error in the correlation peak widths are similar, and are of the form $A/(1 + R)$, where the factor A depends upon the power spectrum of the data. We expect to find a similar result, except that A will be noticeably different for stars with very different rotational velocities.

We have used the synthetically broadened, random noise-added spectra to investigate the errors observed as a function of R. In Figure 2 we show the results of this procedure for a spectrum synthetically broadened to 20 km s^{-1}. Also shown are a large number of repeated observations of T Tauri and DI Cep, for which we measure $v \sin i$ values of 20 and 18 km s^{-1}, respectively. We find excellent agreement between the scatter in the true measurements as a function of R and our noise-added synthetic spectra. The solid curve $\Delta v \sin i = \pm 20/(1 + R)$ km s^{-1} provides a reasonable outer envelope ($\sim$90% confidence limits) for most of the data points.

A similar result is shown in Figure 3, where the results of noise-added synthetic spectra for $v \sin i = 50$ and 60 km s^{-1} are compared with the scatter observed for the rapidly rotating stars SU Aur and RY Tau. Again the agreement between the random noise tests and the scatter in observations is good. The envelope curves are given by $\pm 50/(1 + R)$ km s^{-1}, satisfying the expectation that the scaling of the error should vary linearly with the typical frequencies present in the data (see Tonry and Davis 1979) and therefore should be proportional to $v \sin i$. Therefore, we estimate our 90% confidence level of a $v \sin i$ measurement at $\pm v \sin i/(1 + R)$.

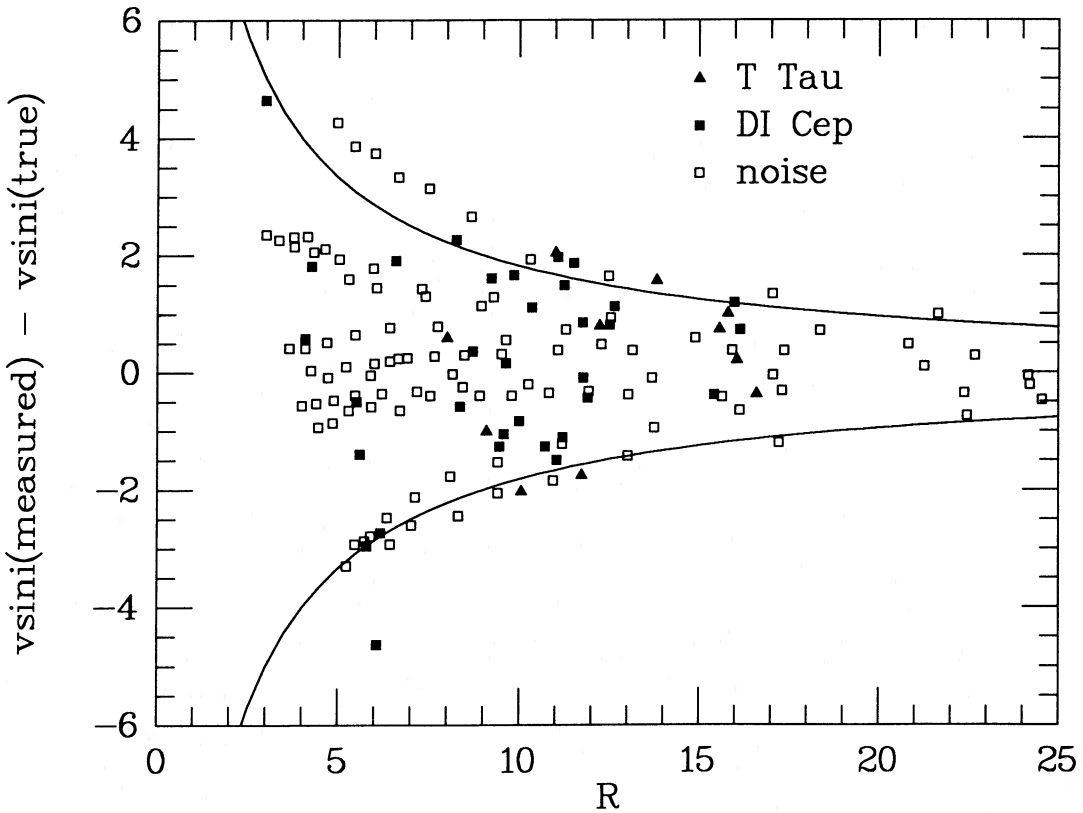

FIG. 2.—Scatter plot for $v \sin i$ vs. R. Open squares are individual results for a spectrum synthetically broadened to 20 km s^{-1} to which different amounts of random noise have been added. Results for T Tau and DI Cep are also plotted, where the ordinate is the difference of individual $v \sin i$ measurements from the mean. Smooth curves denote the relation ± 20 km s$^{-1}/(1 + R)$.

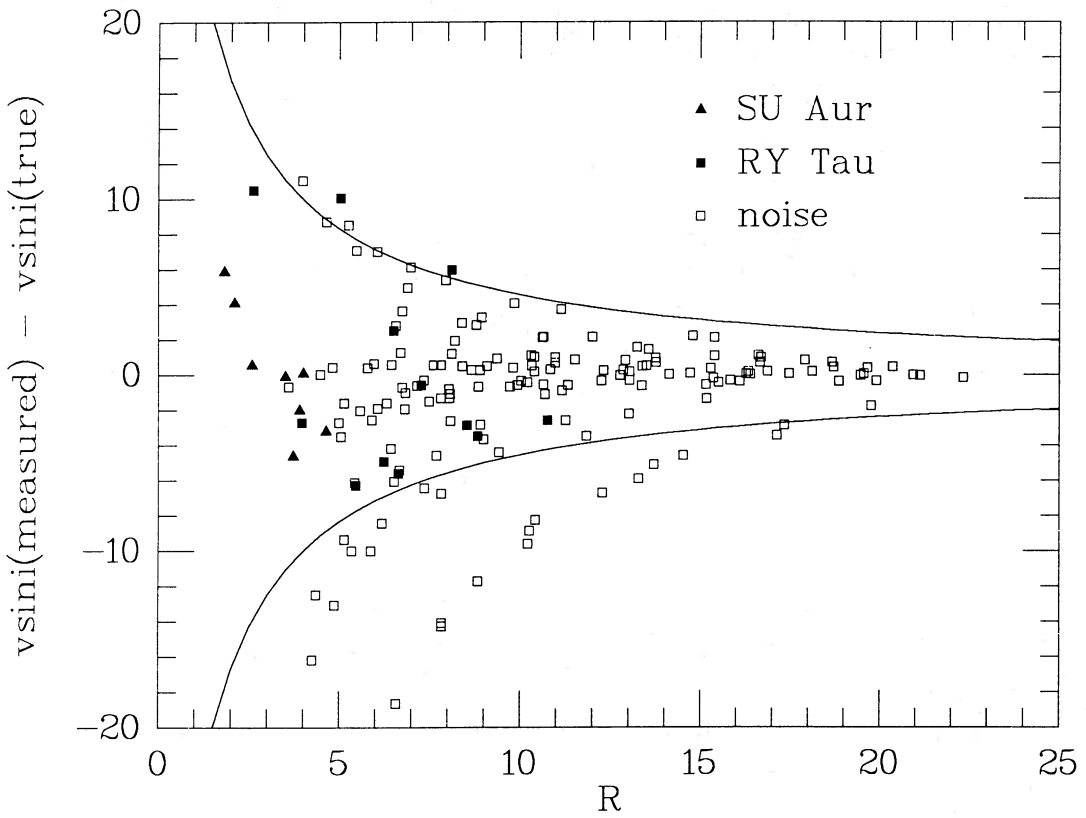

FIG. 3.—Scatter plot of $v \sin i$ vs. R for rapidly rotating stars. Open squares are results for spectra synthetically broadened to 50 and 60 km s^{-1} with varying amounts of random noise added. Results for the rapid rotators RY Tau and SU Aur are plotted as differences from the mean. Smooth curves denote the relation ± 50 km s$^{-1}/(1 + R)$.

The above discussion deals only with random errors. The most likely source of systematic errors is template mismatch. We have conducted tests using G, K, and M dwarf spectra as templates. The difference in derived rotational velocities produced by using different spectral type templates is less than 10%, and is only measurable at the lowest velocities. Because our random rotational velocity errors are generally $\sim 10\%$ or more, we have neglected this effect and have used a K5 dwarf template for the program stars discussed here.

The most worrisome template mismatch occurs when a T Tauri star has an excessively peculiar spectrum. Because we subtract the continuum level before analysis, the addition of continuous emission (with no spectral features in our bandpass) should not affect our results. Chromospheric emission reversals, like the one observed in the Mg I λ5183 line in DI Cep, are another story. As discussed above, our analysis procedures ensure that the Mg I line does not have much effect on our correlations. Furthermore, Mg I emission is not generally strong; thus we presume that the emission effects in the much weaker photospheric lines on which our analysis is based should be relatively unimportant.

A few stars have obviously peculiar spectra. We discuss one special case, RW Aur, in more detail below. Since all methods of measuring rotational velocities depend upon comparison with some standard, there does not seem to be an obvious way around the template mismatch problem.

Another possible difficulty results from interpreting an unresolved double-lined spectroscopic binary as a rapid rotator. There is not much we can do about this for stars where we have no repeat spectra. In a few cases the correlations appear double-peaked; we have removed these stars from the analysis, and will present further discussion of these data in a future paper. In any event, one should keep in mind that our measured rotational velocities for objects with only one observation may be too high if a companion is present.

In Figure 4 we show a comparison between our $v \sin i$ measurements and those of Vogel and Kuhi (1981) for four stars in Tau-Aur and two in NGC 2264. (Results for NGC 2264 will be discussed in a forthcoming paper). Our average error estimates are given by $v \sin i/2(1 + R)$ in cases of single exposures, and are standard deviations in cases where we have repeat exposures. The agreement is good; there is no evidence for a systematic difference between our measurements and those of Vogel and Kuhi, who used photographic image-tube spectra of lower resolution and analyzed the data using power spectrum fitting. In addition, Bouvier and Bertout (1986) are conducting a similar survey of southern T Tauri stars. For several objects in common the agreement is good (Bouvier 1985, private communication).

Radial velocities are also obtained at the same time rotational velocities are measured. In general, tests similar to those discussed previously for rotation indicate comparable errors in rotational and radial velocities. In Figure 5 we show the results of repeat observations and of noise tests analogous to those

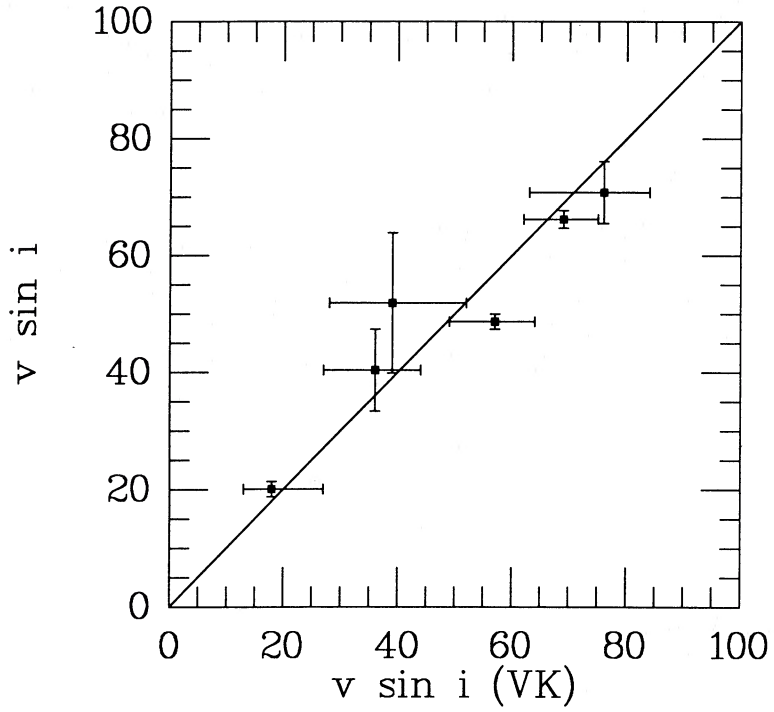

FIG. 4.—Comparison between our $v \sin i$ measurements and those of Vogel and Kuhi (1981) for six stars in common (two from NGC 2264)

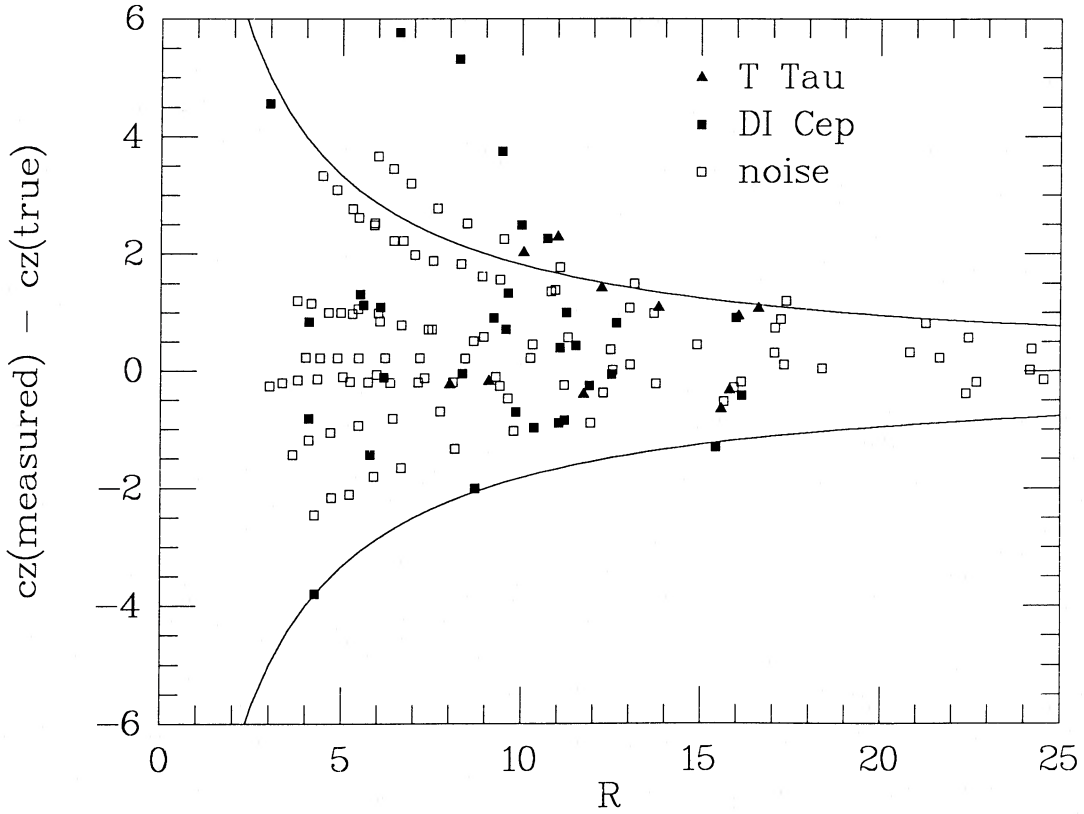

FIG. 5.—Scatter plot for radial velocities, with the same stars and symbols as in Fig. 2

presented in Figure 2 on the measurement of radial velocity. As suggested by Tonry and Davis (1979), the error in radial velocity is similar to the rotational velocity error.

III. ROTATIONAL AND RADIAL VELOCITY RESULTS

a) *Survey Statistics and Results*

We drew our samples of stars from the compillation of Cohen and Kuhi (1979). Adopting the V magnitudes from CK, we observed all 49 late-type stars in Taurus-Auriga down to $V = 14.5$. We also observed another seven out of 16 stars in the range $14.6 \leq V \leq 15.1$. The V magnitude limit is, of course, rather crude, since T Tauri stars are quite variable.

We were not able to obtain velocity measurements for all stars. The blue line and continuum emission of some objects obliterates photospheric lines in our wavelength region, and in some cases the stars were too faint to obtain satisfactory spectra. In addition, the results for the strong-emission star RW Aur are ambiguous, as described below. Thus, we have measured rotational velocities for 35 of the 49 stars brighter than 14.6; overall, 42 out of the 56 stars observed in Tau-Aur have measured velocities.

We also observed 12 out of 20 stars brighter than $V = 13.4$ in the Orion complex (Cohen and Kuhi 1979). We determined rotational velocities for eight of these objects. The Orion stars have generally higher masses than those studied in Tau-Aur. The latest spectral type is K6, so our later discussions of rotation for low-mass stars are based entirely on data from Tau-Aur.

Table 1 presents the basic results of our survey of stars in the Taurus-Auriga clouds and in Orion. The number of usable spectra are given in column (2), along with the range of R values for these spectra in column (3). In columns (4) and (6) we present the mean measured radial velocities and rotational velocities, respectively. We also give the formal standard deviation of a single measurement (1 σ) for cases where we have multiple observations. Our *estimated* average errors, as discussed in the previous section, are about $\pm\, v \sin i/2(1 + R)$ for both rotational and radial velocities. One observes that the repeat measurements are in adequate agreement with this error estimate.

There is uncertainty in combining repeat observations in cases where some spectra indicate $v \sin i < 10$ km s^{-1}, while others suggest rotation at values just above this threshold. We have chosen to average results as if the upper limits were actually detections at 10 km s^{-1}. This procedure was not followed if more than half of repeat observations indicated $v \sin i < 10$ km s^{-1}; in such cases we adopted an upper limit of < 10 km s^{-1}. Care should be employed in interpreting values of $v \sin i$ near our detection threshold.

Our results are in agreement with those of Vogel and Kuhi (1981), who found that most T Tauri stars rotate more slowly than 35 km s^{-1}. We find that almost all of the stars in the Tau-Aur cloud rotate at $v \sin i \lesssim 20$ km s^{-1}.

b) *Comments on Individual Stars*

BP Tau.—Herbig's (1977*a*) study suggested some radial velocity variability; our five spectra of this star provide no additional evidence for this.

RY Tau.—Herbig (1977*a*) found evidence for a radial velocity range of 18 km s^{-1} in this star. The measured dispersion in radial velocity from 10 spectra is consistent with our expected errors $\sim \pm 5$ km s^{-1}.

TABLE 1

ROTATIONAL AND RADIAL VELOCITIES

Object (1)	N (2)	R (3)	V(rad) (4)	ΔV (5)	$v \sin i$ (6)
AA Tau	4	6.4–7.5	16.1 ± 2.1	+0.4	11.0
BP Tau	6	4.0–6.9	15.8 ± 1.0	+0.2	≤10.
CI Tau	3	3.4–4.9	16.4 ± 1.3	−0.1	11.0
CW Tau	2	4.5–6.5	14.5	−1.2	36.
CX Tau	2	3.7–4.9	19.0	...	20.0
CY Tau	1	3.44	19.1	3.1	11.0
DE Tau	3	2.5–3.3	14.9 ± 0.6	−1.2	≤10.
DI Tau	4	5.9–10.4	16.0 ± 0.8	0.0	10.6
DK Tau	2	4.3–5.4	15.3	...	11.5
DM Tau	2	3.1–4.2	16.9	...	≤10.
DN Tau	5	8.2–11.7	16.1 ± 1.6	0.0	≤10.
DO Tau E	2	2.9–4.8	21.2	4.7	13.8
DS Tau	3	2.9–4.0	16.3 ± 2.3	−0.8	≤10.
FX Tau	2	3.5–3.9	16.8	...	≤10.
GG Tau	3	5.3–9.0	17.6 ± 2.2	...	≤10.
GH Tau	3	3.0–5.7	18.4 ± 0.3	1.3	28.3 ± 5.1
GI Tau	4	3.8–6.3	18.1 ± 1.6	1.1	11.6
GK Tau	4	6.6–9.8	18.6 ± 1.4	1.6	16.9 ± 2.9
GO Tau	1	3.5	21.3	...	21.0
Haro 6–37(n)	1	2.7	19.5	...	18.7
Haro 6–37(s)	2	6.2–7.3	23.2	...	10.3
HK Tau	1	3.3	16.3	...	21.8
HK Tau.g2	2	4.3–4.4	18.3	...	24.9
HP Tau	3	4.3–8.2	17.7 ± 1.8	...	14.4 ± 0.8
HP Tau.g2	4	...	...	...	100 ± 20[a]
Hubble 4	6	8.0–15.9	15.0 ± 1.7	−1.3	12.9 ± 2.0
IQ Tau	1	4.9	15.3	...	12.4
LkHa266 N	2	4.4–4.7	20.7	...	16.8
LkHa266 S	1	3.5	20.1	...	15.2
LkHa331	1	2.6	19.6	...	19.2
LkHa332	2	3.3–6.3	15.7	...	≤10.
LkHa332.g2	2	3.8–4.3	14.7	...	20.4
RY Tau	10	6 –10.7	16.5 ± 2.4	0.4	48.7 ± 3.8
T Tau	14	7.8–17.3	19.1 ± 1.2	−0.4	20.1 ± 1.2
UX Tau A	7	9.3–17.8	15.6 ± 3.1[b]	−3.6	24.9 ± 1.7
UX Tau B	2	5.1–7.1	18.7	−0.5	11.7
UZ Tau W	1	4.7	18.5	...	13.5
V410 Tau	8	4.2–9.5	17.8 ± 11.6	1.5:	70.7 ± 9.9
VY Tau	5	5.8–9.8	17.8 ± 1.0	...	≤10.
GM Aur	10	4.6–11.	15.0 ± 1.3	−0.2:	12.8 ± 2.3
RW Aur	13	2.9–7.9	14.0 ± 4.9[c]	...	19.5 ± 6.4[c]
SU Aur	10	3.1–8.8	16.0 ± 3.1	0.7	66.2 ± 4.6
AZ Ori	1	10.1	22.9	...	23.7
BD Ori	1	8.6	22.2	...	47.3
GW Ori	1	4.4	33.6	...	40.4
P1270	1	12.5	26.1	...	15.8
P1404	1	7.2	26.6	−0.2	27.1
San 1	1	6.8	20.1	...	12.0
TX Ori	1	7.4	29.5	...	≤10.
V466 Ori	1	10.4	23.2	...	21.5

NOTES.—Col. (1), object name; col. (2), number of spectra used to determine rotational and radial velocities; col. (3), the signal-to-noise or R values for the spectra, or the range of R values (see text); col. (4), heliocentric radial velocities in km s^{-1}; col. (5), difference of mean radial velocity from nearby molecular cloud velocities given by Herbig 1977; col. (6), $v \sin i$ values in km s^{-1}. Dispersions quoted in cols. (4) and (5) are the *formal* 1 σ dispersions per observation calculated in cases where more than two spectra are available and where upper limits are not averaged in. The 90% confidence limits for the values presented in cols. (4) and (5) are approximately given by $\pm v \sin i/(1 + R)$.

[a] Uncertain measurement.

[b] Radial velocity may be variable.

[c] Variable: see Table 2.

GM Aur.—Our heliocentric radial velocity of 15 km s^{-1} differs considerably from the value of −12 km s^{-1} cited by Herbig (1977*a*), and is quite consistent with the velocity of the associated molecular gas (see below).

DS Tau.—Our radial velocity of 16 km s^{-1} is far from Herbig's (1977*a*) measurement (0 km s^{-1}).

UX Tau.—The radial velocity of the well-observed primary is ~3 km s^{-1} from the velocities of both component B and of the associated molecular cloud (see below), and the dispersion in radial velocity measurements is larger than expected. Our rotational velocity of 25 km s^{-1} for A is in good agreement with Herbig's (1957) estimate of 20–25 km s^{-1}.

RW Aur.—This strong-emission star is known to exhibit unpleasantly large variations in its spectrum. In Figure 6 we present some of our spectra and cross-correlations. At times the spectrum appears to be that of a K star rotating at ~20 km s^{-1}, in fair agreement with the estimate of ~25 km s^{-1} by Mundt and Giampapa (1982), but at other times the region is dominated by strong emission lines and blue continuum. Not all spectra provide believable correlations; however, a number of reasonable-looking correlations indicate radial velocity variability over a range of ~10 km s^{-1} (see Table 2). We tentatively conclude that RW Aur is a multiple system, which may contribute to the peculiarities of the spectrum of this object. With the present set of data it is difficult to infer anything about periods and separations, but changes in radial velocity of a few km s^{-1} occur on time scales of days (Table 2), suggesting a relatively close binary.

P1404.—Our $v \sin i$ value of 27 km s^{-1} differs from the value of 14 km s^{-1} measured by Smith, Beckers, and Barden (1983).

San 1.—This star's position in the H-R diagram according to Cohen and Kuhi (1979) is well above the "birth line" proposed by Stahler (1983). Our spectra are not well suited to obtain spectral types, but the data suggest an earlier spectral type than the M type assigned by Cohen and Kuhi (1979).

c) Comparison with Photometric Rotational Periods

In some cases, periodic light variations have been observed from T Tauri stars (Rydgren and Vrba 1983; Vrba *et al.* 1984; Rydgren *et al.* 1985). These variations have been attributed to

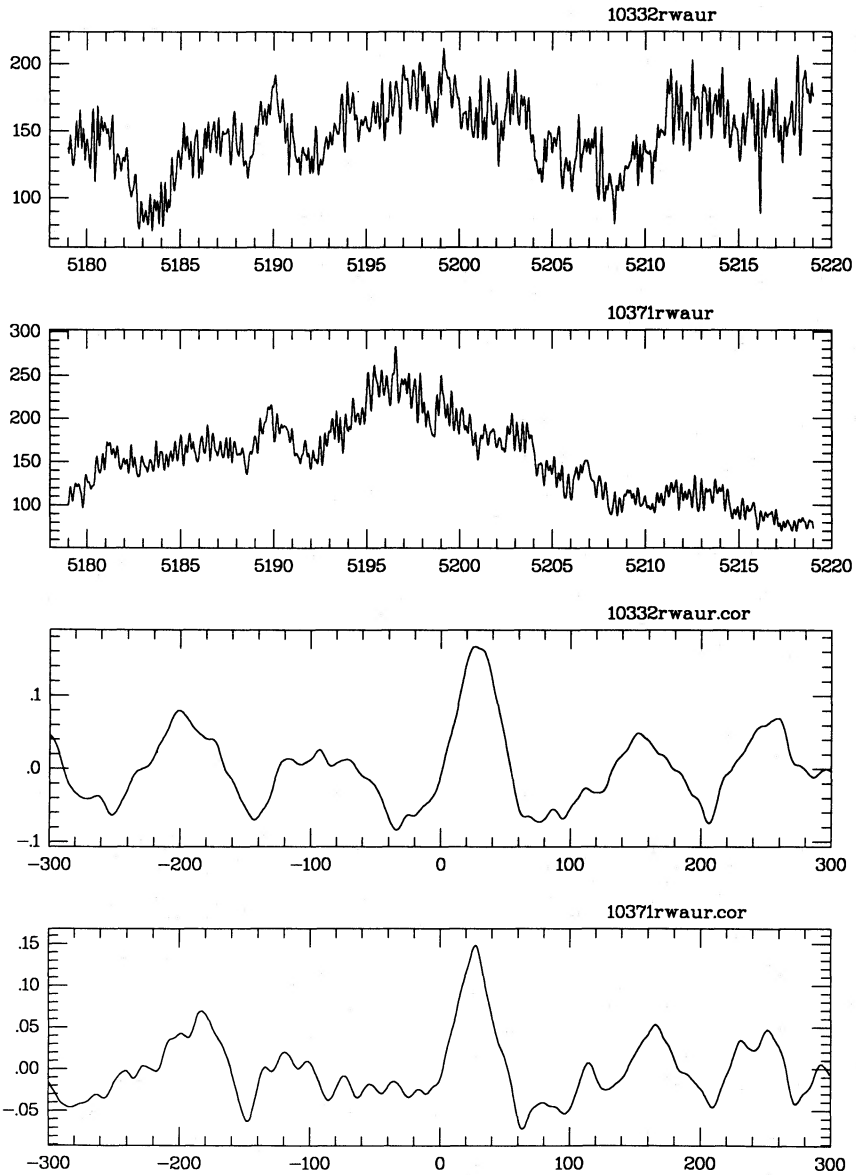

FIG. 6.—Sample spectra and the associated cross-correlations for RW Aur (see text, Table 2)

TABLE 2

OBSERVATIONS OF RW AUR

Spectrum	R	V(rad)	$v \sin i$	JD
4188.....	...	...	...	2,444,918.901
4202.....	...	...	...	2.444.920.006
6024.....	8.0	17.9	15.9	2,445,275.982
6521.....	6.7	12.2	25.9	2,445,981.031
6884.....	3.6	10.0	22.1	2,446,036.988
6933.....	...	...	...	2.446,037.924
7707.....	...	...	...	2,445,630.019
8049.....	...	...	...	2,445,663.997
8236.....	3.9	14.0	13.7	2,445,719.789
10332.....	7.9	15.3	24.8	2,445,984.031
10371.....	5.6	12.7	14.7	2,445,986.968
10390.....	4.4	22.4	23.1	2.445,987.918
10397.....	4.3	20.9	16.0	2,445,988.033
10564.....	2.9	10.4	15.2	2,446,012.816
10588.....	7.1	15.9	13.7	2,446,013.784
10610.....	3.8	7.3	32.8	2,446,014.763
11056.....	2.7	16.0	$\leq 10.$	2,446,102.750
11064.....	2.8	12.6	12.0	2,446,103.727
11095.....	...	...	...	2,446,104.763

rotational modulation by spots on or near the photosphere. Thus, rotation can be measured without the ambiguity introduced by sin i, if the stellar radii can be estimated. We adopt effective temperatures and luminosities from the compilation of Cohen and Kuhi (1979).

A comparison between the photometrically derived equatorial velocity and our measured v sin i for six of the program stars is shown in Figure 7. The agreement is quite good for the rapid rotator V410 Tau; our crude estimate for HP Tau/G2 also appears reasonable. There is some tendency for our measurements of the slow rotators BP Tau and DN Tau to fall below the equatorial velocities inferred from the photometric periods. We think that our systematic errors in the absolute value of v sin i are no more than 10%, and so the discrepancy is somewhat worrisome. (We have not included GI and GK Tau, two stars with periods reported by Vrba *et al.* 1984 and Rydgren *et al.* 1985. The detailed photometry does not convincingly demonstrate true periodicity.)

d) Radial Velocities

In Table 1 we summarize our radial velocity results. For the 21 stars with multiple observations the rms dispersions of the observations are also presented. Typically the simple measurement error is on the order of 1.5 km s^{-1} for slowly rotating stars, with larger errors for rapid rotators as discussed previously. Our radial velocities are generally consistent with Herbig's (1977*a*) results, to the level of his error estimate ~ 4 km s^{-1}. However, we note that our results for GM Aur and DS Tau are very different.

Herbig (1977*a*) showed that T Tauri stars are closely associated kinematically with neighboring molecular cloud material. From an analysis of 26 stars Herbig found that the mean velocity of the stars relative to molecular cloud velocities measured at the optical position of each T Tauri star was 0.4 ± 0.5 km s^{-1}, with a dispersion of 3.9 km s^{-1}, consistent with his measurement errors.

Herbig presented molecular cloud velocities for 20 of the stars which we have observed in Taurus-Auriga (omitting V410 Tau, for which our measurement accuracy is poor). The velocity differences are given in Table 1, in the sense of stellar velocity minus molecular cloud velocity. The mean velocity difference for the entire sample is 0.2 ± 0.4 km s^{-1}; the dispersion of individual stars about the mean is 1.7 km s^{-1}. Three stars have velocity differences much larger than this dispersion. The value for CY Tau is based on only one measurement. DO

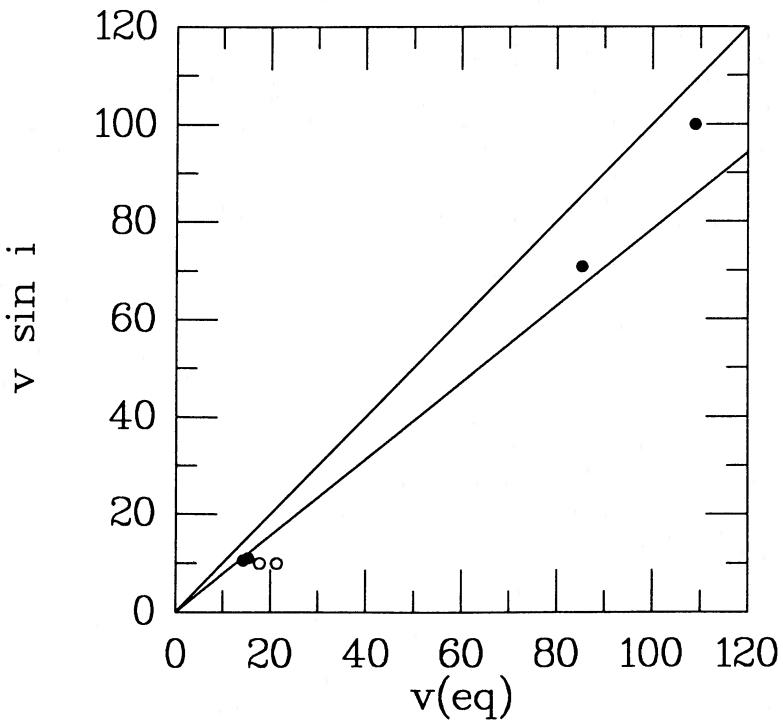

FIG. 7.—Comparison of measured v sin i values with equatorial rotational velocities predicted from photometric periods. Open symbols denote v sin i upper limits. Straight lines mark the relations $v \sin i = v(\text{eq})$ and $v \sin i = (\pi/4)\, v(\text{eq})$.

Tau E is 4.7 km s^{-1} from the molecular cloud velocity, an unexpectedly large difference given the estimated quality of the radial velocity measurement. The mean of several exposures for UX Tau A is -3.6 km s^{-1} from the cloud velocity, and the dispersion of 3.1 km s^{-1} is also large. Interestingly enough, our radial velocity for UX Tau B is essentially at the cloud velocity, which suggests that A may be a spectroscopic binary. Our radial velocities for CI Tau, GH Tau, DS Tau, GM Aur, RY Tau, and SU Aur are much closer to the cloud velocity than Herbig's values. The true stellar dispersion is clearly comparable to or less than our measurement errors, and we can say only that the true relative velocity dispersion between molecular clouds and young stars is of order 1 km s^{-1} or less.

Jones and Herbig (1979) estimated the global stellar velocity dispersion in the Taurus-Auriga region to be 2–3 km s^{-1} from proper motion studies. They found smaller velocity dispersions (less than 1–2 km s^{-1}) for tightly concentrated groups of stars. We find a global velocity dispersion for our sample of 2.1 ± 0.3 km s^{-1} (38 stars). If we divide our sample according to the spatial location of stars in the same manner as Jones and Herbig, we have enough stars only in one group to make a meaningful comparison. For objects in the vicinity of group II we find a velocity dispersion of 1.8 ± 0.5 km s^{-1} (16 stars). For the more centrally condensed subset of stars called group IIa by Jones and Herbig, we find a dispersion of 1.3 ± 0.4 km s^{-1} (10 stars). Both values are close to our expected errors, and we conclude that the real velocity dispersions are $\lesssim 1.5$ km s^{-1}. The velocity dispersions of the molecular gas associated with a group (i.e., the point-to-point dispersion as determined by the molecular line velocities given by Herbig 1977) are less than 0.5 km s^{-1}, well below our measurement errors.

Jones and Herbig also found systematic tangential velocity differences between their three groups of 4–5 km s^{-1}. Our mean LSR radial velocities are 7.0 ± 0.9 km s^{-1} for stars in the area of group I (five stars), 7.4 ± 0.5 km s^{-1} for group II (16 stars), and 6.7 ± 0.8 km s^{-1} for group II (five stars; including UX Tau A, the result is 6.2 ± 0.8 km s^{-1}). The quoted errors are formal dispersions of the mean. These results are consistent with the associated molecular gas velocities (averaging over the observations in the directions of T Tauri stars in each group given by Herbig) of 7.0, 6.2, and 7.2 (one observation) km s^{-1}, respectively. Clearly there are no systematic radial velocity differences among the groups at the same level as the tangential velocity differences reported by Jones and Herbig.

The kinematic picture of the Taurus-Auriga region derived from our radial velocities then is similar to that presented by Herbig (1977) and Jones and Herbig (1979) based on somewhat less precise velocities. There is no evidence for any systematic velocity differences between the stars and the gas. The dispersion of the stellar motions relative to the gas is $\lesssim 1.5$ km s^{-1}. This dispersion is consistent with the internal motions of the gas (Ungerechts and Thaddeus 1986). We find no evidence for relative motions between the concentrations of T Tauri stars at the level of 2 km s^{-1} or greater.

e) Membership Considerations

One concern in interpreting the results of our survey is the possibility that foreground stars might be mistaken for true association members. The strength of Hα emission precludes any uncertainty in identifying many T Tauri stars. However, a significant number of stars in the Cohen-Kuhi list have relatively small Hα equivalent widths, comparable to the emission observed from dMe stars.

In our sample 13 stars later than K6 have Hα equivalent widths less than 10 Å according to Cohen and Kuhi (1979), placing them in the dMe range (Stauffer and Hartmann 1986). High-dispersion spectra of DO Tau E, FX Tau, Hubble 4, LkHα 332/g2, UX Tau A, and V410 Tau clearly show broad Hα emission incompatible with typical dMe spectra. There is some evidence for broad Hα wings in VY Tau, and this object is known to undergo five magnitude outbursts in light (Herbig 1977*b*), decidedly uncharacteristic of dMe stars.

Of the six remaining weak Hα stars, three have rotational velocities greater than 15 km s^{-1}, atypical of dMe stars (Stauffer and Hartmann 1986). This leaves UX Tau B, DI Tau, and IQ Tau. UX Tau B is very probably associated with UX Tau A, and has a radial velocity within 1 km s^{-1} of the neighboring molecular material. DI Tau has a radial velocity right at the velocity of neighboring molecular material, and its placement close to the strong-emission star DH Tau suggests they are a physical pair. IQ Tau is located near DI Tau and has a radial velocity within 1 km s^{-1} of DI Tau. Thus, we have no evidence for foreground contamination in our T Tauri survey.

IV. ROTATIONAL VELOCITY DISTRIBUTIONS

a) Overview of Pre–Main-Sequence Rotation

In Figure 8 we show our program stars in Taurus-Auriga and in Orion placed on an H-R diagram. The evolutionary tracks are the same as adopted by Cohen and Kuhi (1979). As reported by Vogel and Kuhi (1981), high-mass stars on their radiative tracks are more often rapid rotators than low-mass stars. V410 Tau, assigned a spectral type of K7 by Cohen and Kuhi (1979), appears to be one rapid rotator with $M < 1\ M_\odot$. However, Rydgren and Vrba (private communication) classify V410 Tau as K3–K5, which would suggest a mass greater than $1\ M_\odot$.

We have found rotation above our detection limit of 10 km s^{-1} in 24 of the 32 program stars with good spectra that have estimated masses less than $1\ M_\odot$. Four of the program stars with upper limits have inferred equatorial velocities ~ 15–20 km s^{-1} from photometric periods (Vrba *et al.* 1984; Rydgren *et al.* 1985). Thus the rotational velocities of the great majority of low-mass T Tauri stars are $\lesssim 20$ km s^{-1}. The principal remaining uncertainty arises from the absence of results for strong emission-line stars.

b) Distribution of Rotational Velocities among Low-Mass T Tauri Stars

We now consider the distribution of pre–main-sequence rotational velocities in more detail, restricting our attention to T Tauri stars with masses less than $1\ M_\odot$, where we have the most data. In order to construct statistically meaningful samples it is necessary to bin the data in mass ranges. We have chosen to consider the $0.7 \lesssim M/M_\odot \lesssim 0.9$ stars as a group, since it appears difficult to segregate objects by mass in this interval. Small uncertainties in assigning spectral types can produce large errors in the assigned mass because the evolutionary tracks for different masses are quite close together in the relevant region of the H-R diagram. We also choose, somewhat arbitrarily, another mass bin of 0.5–$0.4\ M_\odot$.

In Figure 9 we display rotational velocities for these two groups of stars plotted against stellar radii derived from the bolometric luminosities and effective temperatures estimated by Cohen and Kuhi (1979). The lower mass stars have systematically larger rotational velocities at a given radius.

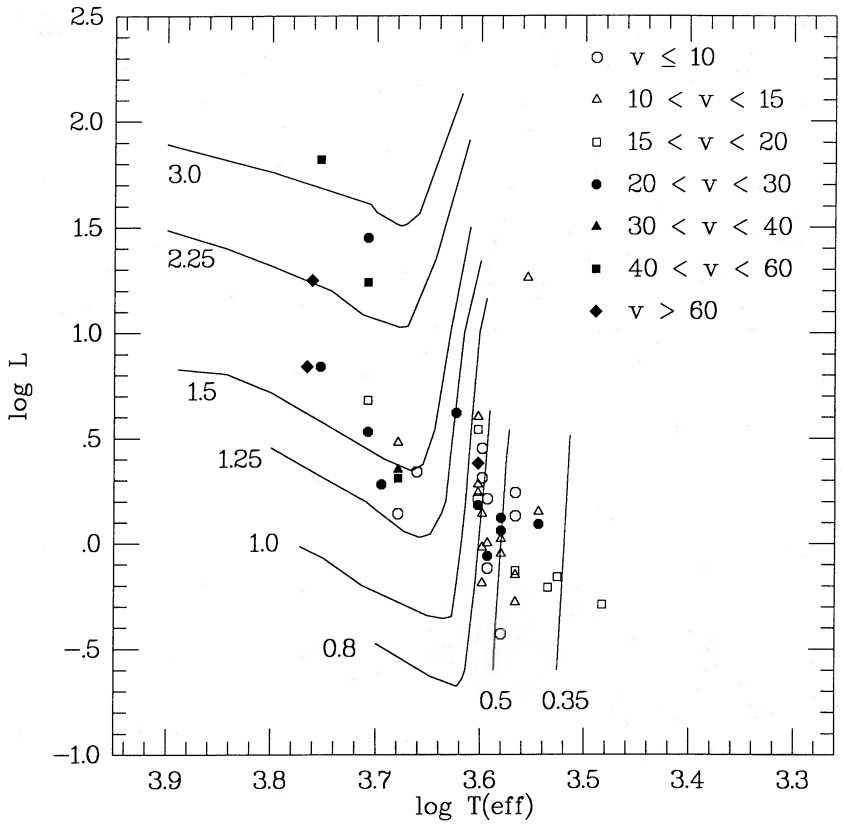

FIG. 8.—Rotational velocities of T Tauri stars, located in the H-R diagram according to Cohen and Kuhi (1979)

As shown in Figure 9, there are too few stars in our mass bins at a given radius to determine a meaningful rotational velocity distribution. To make further progress, we have estimated the rotation rates that stars would have at a common radius and analyze the resulting distribution of $v \sin i$. Our estimated rotational velocities assume that stars contract homologously and conserve angular momentum in this region of the H-R diagram. The assumption of homologous contraction should be good for these completely convective stars. The data are too sparse to prove that angular momentum is conserved in the relevant range of radii. However, we show below that the accumulated angular momentum loss during the entire phase of pre–main-sequence contraction is relatively modest, so that the assumption of angular momentum conservation in our restricted region of the H-R diagram may not be too bad.

Because our data contain upper limits, we use the Kaplan-Meier maximum likelihood technique to estimate the true distributions (Avni *et al.* 1980; Feigelson and Nelson 1985). The cumulative rotational velocity distributions (projected to a common radius) derived for our two mass groups are shown in Figure 10. Each group contains the same number of stars (13), and the distributions are normalized to the maximum observed $v \sin i$ in each mass range.

The observed rotational velocity distributions shown in Figure 10 have a striking concentration of stars at low $v \sin i / v \sin i$ (max). These distributions are different from that which would result from all stars having the same rotation at the same radius, but a random distribution of sin i, in which case the distribution should be peaked at high velocities. The latter distribution is also shown in Figure 10. Rank tests of the cumulative distribution functions show that the probability that the observed distributions are consistent with the zero velocity spread distribution is less than 10% for both mass ranges, and χ^2 tests show that the zero velocity spread model is a very poor fit to the data (binning the upper limits together; Lawless 1982). These statements are insensitive to reasonable modifications in the adopted normalizing factors $v \sin i$ (maximum). Thus, if our assumption of minimal braking during the T Tauri phase is correct, and if sin i is distributed randomly, we conclude that stars within each mass range do not all have the same angular momentum. This spread in angular momentum must reflect a corresponding spread in initial conditions.

Figure 10 indicates a systematic difference between the observed distributions in the two mass ranges. This difference has been exaggerated, however, by the specific normalization chosen. If we normalize the observed distributions instead by their mean, rank tests indicate no significant difference.

c) Comparison with Main-Sequence Rotational Velocity Distributions

Recent studies of young open clusters shows that many solar-type stars are rapidly rotating when they first arrive on the main sequence (Stauffer *et al.* 1984, 1985). In Figure 11*a* we show rotational velocities derived by Stauffer *et al.* (1985) for 0.5–1.0 $M_\odot$ stars in the youngest ($t \approx 5 \times 10^7$ yr) well-studied open cluster, α Per. (We have chosen not to compare our data with measured rotation for the Pleiades cluster [Stauffer *et al.* 1985] because main-sequence angular momentum loss has clearly occurred to a much greater extent in this older cluster than in α Per.) The observed rotational velocities of T Tauri stars in the same mass range (Fig. 11*b*) imply that at least some

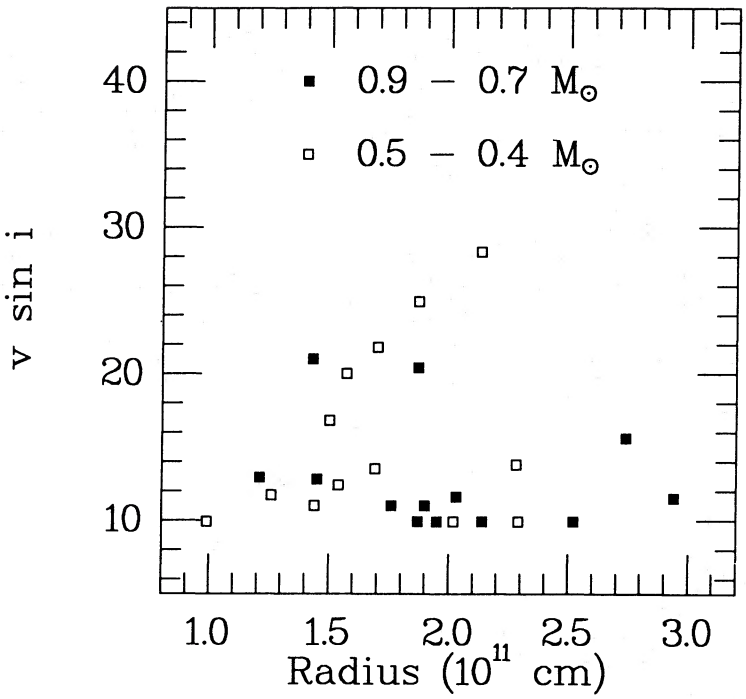

FIG. 9.—Distribution of $v \sin i$ values for T Tauri stars vs. the stellar radius, for two mass ranges

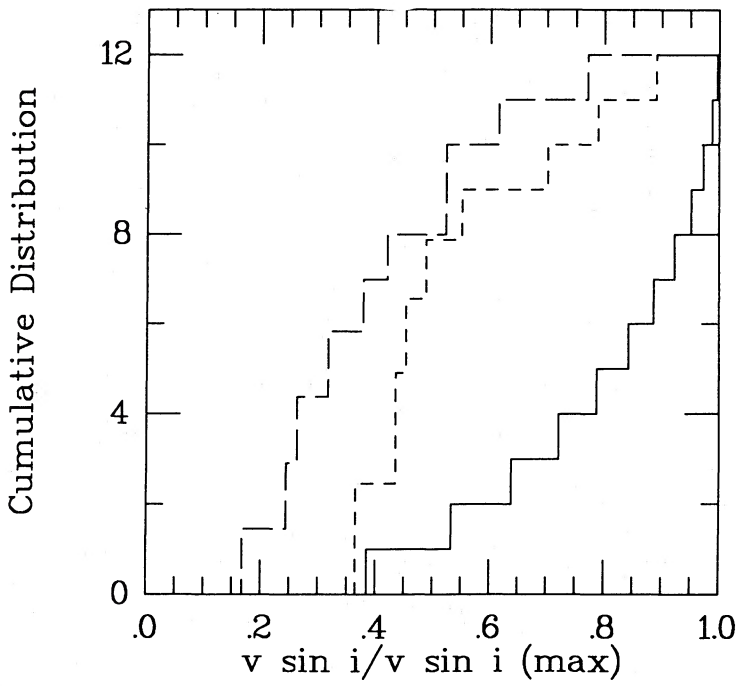

FIG. 10.—Maximum likelihood cumulative distributions as a function of normalized $v \sin i$, compared with that expected from a model in which the stars in a given mass bin have the same rotational velocity at a given radius, but have a random distribution of sin i. Solid line indicates the zero velocity spread, random sin i model distribution; short dashed line indicates the distribution for stars in the range 0.7–0.9 $M_\odot$, and long dashed line denotes stars in the range 0.4–0.5 $M_\odot$.

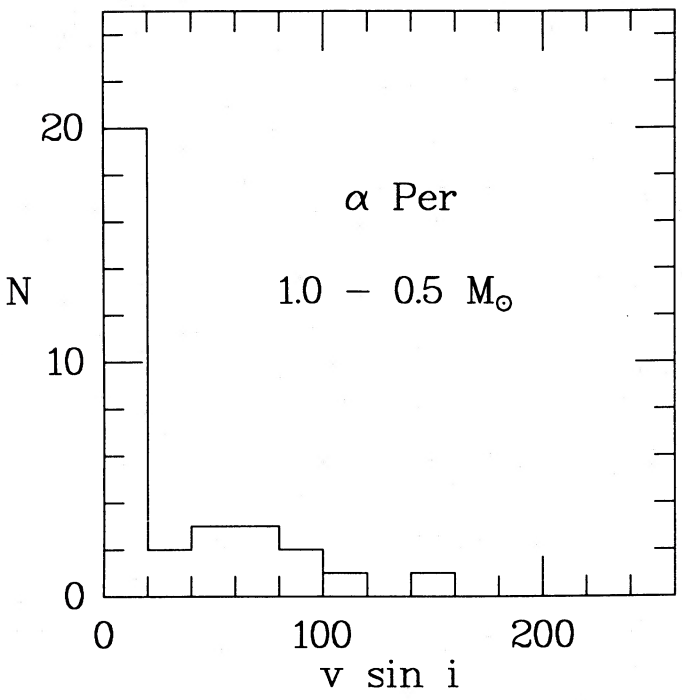

FIG. 11*a*

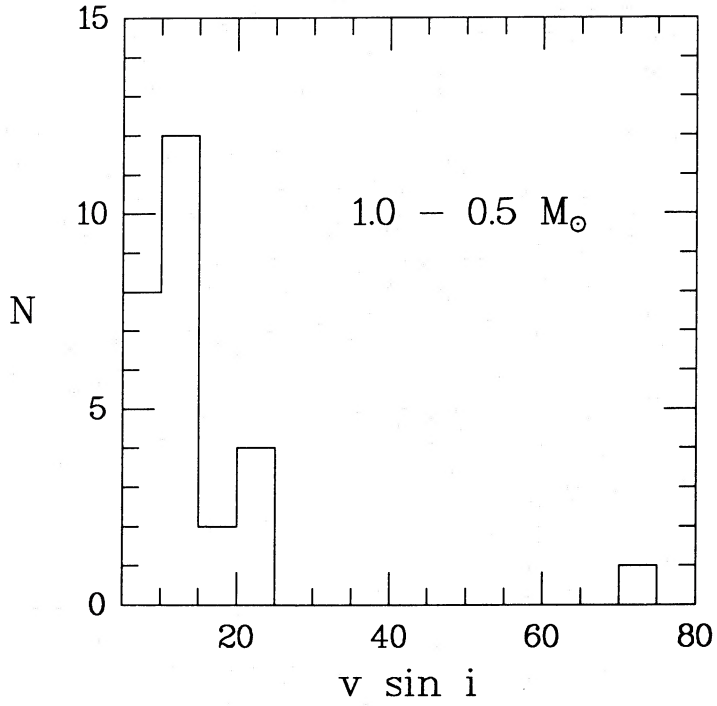

FIG. 11*b*

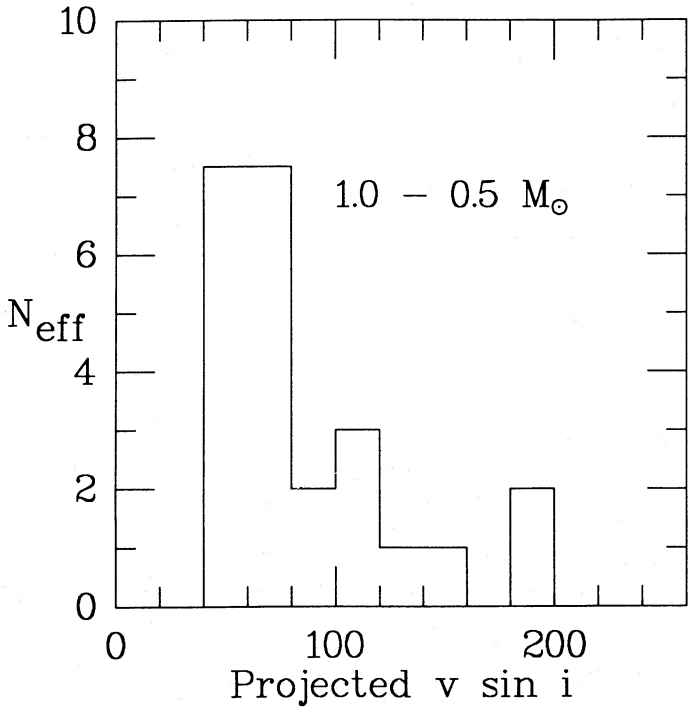

FIG. 11*c*

FIG. 11.—(*a*) Distribution of $v \sin i$ for stars in the α Per cluster in the mass range 0.5–1.0 $M_\odot$ (Stauffer *et al.* 1985). (*b*) Observed distribution of $v \sin i$ for T Tauri stars in the same mass range. (*c*) Distribution of zero-age main-sequence $v \sin i$ values for the stars in (*b*), projected assuming solid-body rotation and conservation of angular momentum. The Kaplan-Meier maximum likelihood estimator has been used to include upper limits in this binned representation of the data (see text).

T Tauri stars spin up during contraction to the main sequence. These data can be used to constrain the amount of angular momentum lost during the pre–main-sequence evolution of low-mass stars.

Using the bolometric luminosities, effective temperatures, and pre–main-sequence tracks of Cohen and Kuhi (1979) to assign masses and radii to our program stars, we have calculated the zero-age main-sequence rotational velocities of these stars assuming conservation of angular momentum and solid-body rotation. Moments of inertia for this calculation were interpolated from the results presented by Gilliland (1985). The main-sequence rotational velocity distribution projected in this way is shown in Figure 11*c*, using the standard maximum likelihood technique to correct for the effects of upper limits (Avni *et al.* 1980; Feigelson and Nelson 1985). We have left out the rapid rotator in Figure 11*b*, V410 Tau, because other observations suggest it has a mass greater than 1 $M_\odot$ (see § IV*a*). Clearly the slowly rotating T Tauri stars can become sufficiently rapid rotators on the ZAMS to explain the open cluster observations.

Figure 11*c* shows that a reduction of a factor of 4 in the angular momentum of the T Tauri distribution would roughly reproduce the low-velocity peak in the α Per distribution. However, a universal reduction in T Tauri angular momentum by this factor would not leave enough rapid rotators to account for the high-velocity end of the α Per distribution. If one supposes that the angular momentum loss for all stars is the same, independent of the initial angular momentum, it is possible to produce an appropriate low-velocity peak on the main sequence while still leaving enough rapidly rotating stars.

There are two reasons to think that the factor of 4 reduction in angular momentum implied by the above comparison is an upper limit to the true pre–main-sequence angular momentum loss. First, the low rotational velocity peak in α Per may be exaggerated by rapid main-sequence spin-down; rapid angular momentum loss for G dwarfs on the main sequence is suggested by from comparisons between the α Per and the Pleiades clusters (Stauffer *et al.* 1984). Second, if the calculations of Endal and Sofia (1981) are any guide, magnetic wind braking will first spin down the outer convective envelope, while the radiative core remains more rapidly rotating. In other words, it may not be necessary to spin down the entire star at first in order to produce a lowered surface rotational velocity. We conservatively estimate that less than three-fourths of the angular momentum of a typical T Tauri star is lost during pre–main-sequence contraction.

Remarkably, both a α Per and the projected T Tauri $v \sin i$ distributions are qualitatively similar, in that both are skewed toward low velocities. Stauffer *et al.* (1985) suggested that the low-velocity peak in α Per might be enhanced by a combination of main-sequence spin-down and noncoeval star formation. If the cluster contains older stars which have more time to spin down, a large population of slow rotators would result. Our data suggest that the low-velocity peak may result more from the initial distribution of stellar angular momentum than from noncoeval star formation in open clusters.

This discussion assumes that the rotational velocities of our sample of T Tauri stars are representative of the entire population. The principal bias we have identified in our survey is the absence of the strong emission-line stars. The strong emission star RW Aur does not appear to have a large projected rotational velocity. In addition, we are at present undertaking rotational and radial velocity studies at longer wavelengths, where emission is less of a problem; preliminary results also indicate that the strong emission stars are not particularly rapid rotators (Hartmann *et al.* 1986, in preparation). Also, we have been unable to discover any connection between rotation and emission among the stars in our sample (see § V*c*). For these reasons we do not think that the absence of strong emission-line stars substantially biases our sample.

In the case of high-mass T Tauri stars (1–3 $M_\odot$), the wider separation of evolutionary tracks in the H-R diagram makes the assignment of mass more secure than for low-mass stars. To calculate the projected ZAMS values of $v \sin i$, we initially assumed solid-body rotation. The results of this procedure are shown in Figure 12*a*. The main-sequence values of $v \sin i$ have been taken from Kraft (1967) and Abt and Hunter (1962). One observes that our projected velocities are very much higher than observed main-sequence values. Either substantial angular momentum loss occurs on the radiative tracks, or the assumption of solid-body rotation is incorrect, or both. Differential rotation during contraction may become more pronounced in high-mass stars than in low-mass objects, because the former have larger radiative zones and smaller convective regions. As another limit, we have also calculated the projected main-sequence rotational velocities, assuming no transfer of angular momentum across radial shells; i.e., $v \sin i \approx 1/R$. As shown in Figure 12*b*, this assumption produces better agreement with main-sequence averages of $v \sin i$. Vogel and Kuhi (1981) also calculated main sequence $v \sin i$ values with this assumption and found rotational velocities somewhat lower than the main-sequence observations. We find somewhat higher projected velocities. Perhaps the Vogel and Kuhi sample of the higher mass stars in NGC 2264 included some nonmembers, which would be preferentially slow rotators.

V. DISCUSSION

a) Angular Momentum and Protostellar Collapse

Low-mass stars rotate at rates far below breakup velocity at an early age. To understand the significance of this result, we should consider the rotation of the parent molecular clouds. It is now widely believed that low-mass stars form in the interiors of dense molecular cloud cores embedded in larger complexes (Myers and Benson 1983). Although a systematic study of their rotation has yet to be undertaken, molecular line observations of most cores fail to show a shift in line center across the core comparable to the intrinsic line width, indicating angular velocities of $\lesssim 10^{-14}$ s^{-1} (Myers and Benson 1983). Since cores have typical densities $\sim 10^4$ cm^{-3} and radii ~ 0.1 pc, their surface rotational velocities are at most 10^{-2} of breakup. Such slow rotation could result from efficient magnetic coupling to the ambient cloud complexes (Mouschovias 1977), especially since these complexes also exhibit angular velocities of the same order of magnitude (Goldsmith and Arquilla 1985).

The gravitational collapse of such slowly rotating cloud cores results in a substantial fraction of the mass being incorporated in a central star, with the remaining material of higher specific angular momentum forming a circumstellar disk (Terebey, Shu, and Cassen 1984). If magnetic braking is inefficient during this protostellar phase, then the collapse of cloud cores with higher initial rotation rates results in almost all the mass being accreted onto a disk. The condensation of a central star in this case is more problematic, and relies on an efficient mechanism for the outward transport of angular momentum (e.g., Larson 1984). The important point is that in *either*

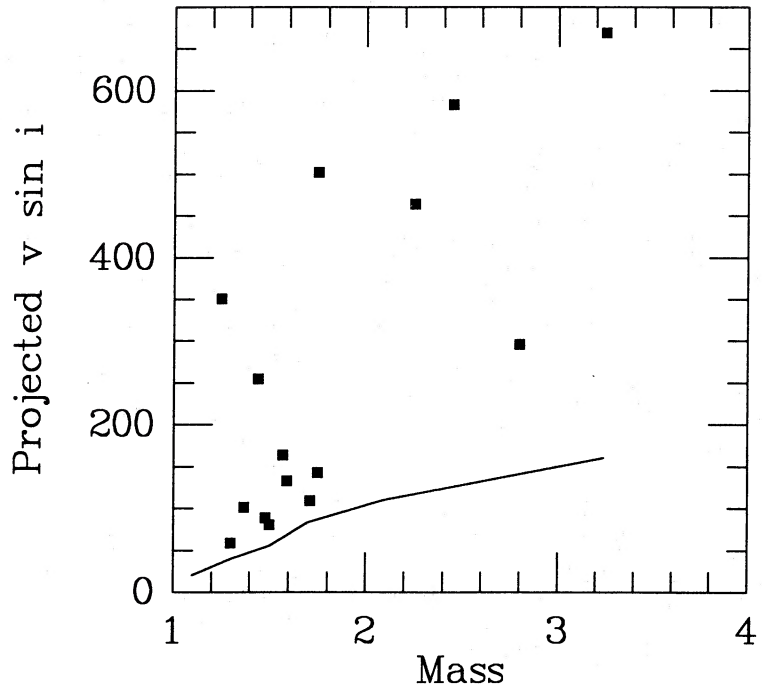

FIG. 12*a*

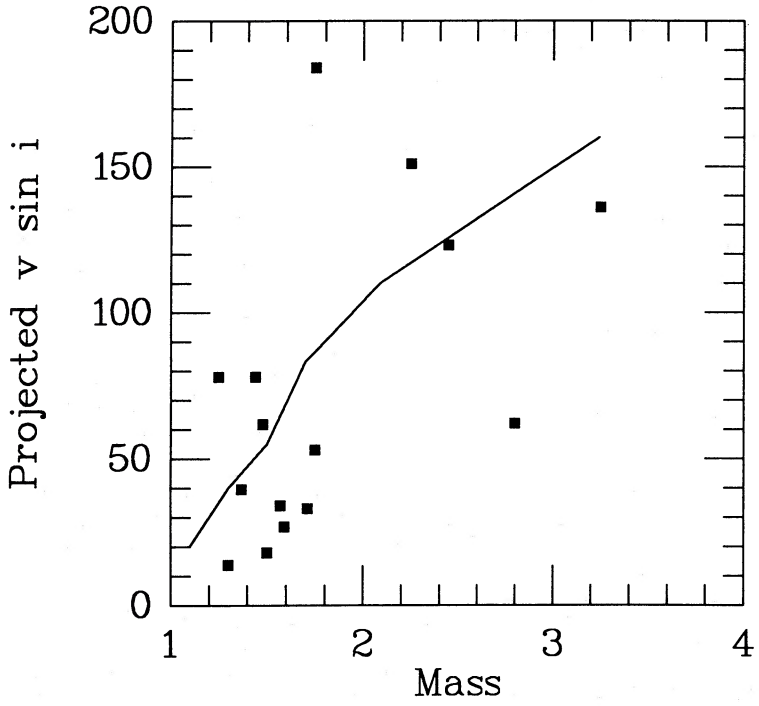

FIG. 12*b*

FIG. 12.—Projected main-sequence velocities for high-mass T Tauri stars, as a function of mass in solar units. Solid line is an average main-sequence rotational velocity relation taken from Kraft (1967) and Abt and Hunter (1962). (*a*) Projected velocities assuming solid-body rotation and conservation of angular momentum. (*b*) Projected velocities assuming $v \sin i \approx 1/R_*$.

picture, the surface velocities of stars which have just ended their protostellar accretion phase should be comparable to breakup speed. For a 1 $M_\odot$ star with a protostellar radius of 5 $R_\odot$ (Stahler, Shu, and Taam 1980), breakup speed is 200 km s^{-1}.

Many of our program stars of subsolar mass have positions in the H-R diagram on or near the stellar "birth line," i.e. the locus of stars immediately following their visually obscured protostellar accretion phase (Stahler 1983). These stars cannot have been undergoing pre–main-sequence contraction for much longer than their Kelvin-Helmholtz ages of $\sim 10^5$ yr. Since almost all rotate at 20 km s^{-1} or less, they have only $\sim 10\%$ of the angular momentum predicted by theories which ignore angular momentum transport during collapse. These stars must therefore undergo substantial braking during or immediately following the protostellar accretion phase; the pre–main-sequence braking cannot last longer than $\sim 10^5$ yr.

It has long been appreciated that fragmentation of the parent molecular cloud could alleviate the spin-up problem by depositing most of the initial angular momentum in orbital motion of the fragments (e.g., Ostriker 1970). Let us briefly consider binary formation in a molecular cloud core. If we idealize the core's structure as a rigidly rotating singular isothermal sphere, then its angular momentum is $(\frac{2}{9})M_c R_c^2 \Omega_c$, where M_c, R_c, and Ω_c are the core's mass, radius, and angular velocity, respectively. Suppose that two collapsing protostars form within this cloud, and that these protostars eventually accrete the entire cloud mass. Now the spin angular momentum of each star of mass $M_c/2$ following accretion is given by $\alpha(M_c/2)R_* V_*$, where R_* and V_* are the protostellar radius and surface velocity, respectively, and α is a dimensionless factor which has the value 0.205 for a fully convective protostar of approximately solar mass. If a fraction ϵ of the initial angular momentum ends up in the spin of each protostar, then V_* is given by

$$V_* = \frac{4\epsilon}{9\alpha}\frac{R_c^2}{R_*}\Omega_c = 5.6 \times 10^4 \text{ km s}^{-1}\, \epsilon \left(\frac{R_c}{0.1 \text{ pc}}\right)^2 \left(\frac{R_*}{5\ R_\odot}\right)^{-1} \left(\frac{\Omega_c}{10^{-14}\ \text{s}^{-1}}\right).$$

Bodenheimer (1978) has suggested a value of 0.1 for ϵ, based on numerical collapse calculations. However, we see that even for ϵ as low as 10^{-2}, V_* formally exceeds breakup speed, implying that V_* will actually equal breakup and that some incoming material must orbit the star in a disk. It is unlikely, therefore, that binary formation per se will result in low surface velocities for newly formed stars. What is needed is rapid angular momentum transport, i.e. braking, in the protostellar or early pre–main-sequence phase.

In the mass range 0.7–1.5 $M_\odot$, our stars have angular momenta per unit mass J between 2.8×10^{16} and 1.7×10^{17} $cm^2\ s^{-1}$ (using a factor of $\pi/4$ to correct for the average sin i). The same quantity for the Sun is $\sim 8 \times 10^{14}$ $cm^2\ s^{-1}$, assuming solid-body rotation (see Brandt, Wolff, and Cassinelli 1969). Thus, solar-type T Tauri stars have angular momenta $\sim$30–200 times that of the present Sun, in rough agreement with the relation $J \approx M^{0.6}$ obtained for higher mass stars (Kraft 1970). It is striking that most of these stars have angular momenta well below the value of 1.6×10^{17} $cm^2\ s^{-1}$ for the present-day solar system (Kraft 1970). Our results suggest that the Sun never had most of the angular momentum of the solar system.

b) Magnetic Braking during Pre–Main-Sequence Contraction

Comparison of the observed projected rotational velocities of T Tauri stars with rotational velocities of similar mass stars when they first arrive on the main sequence allows us to constrain the magnitude of pre–main-sequence angular momentum loss. Our upper limit of a factor of 4 to the angular momentum loss during pre–main-sequence contraction implies that the braking time for stellar wind spin-down cannot be significantly shorter than the Kelvin-Helmholtz time for these stars ($\sim 10^6$ yr). Atmospheric models suggest mass-loss rates $\sim 10^{-8}\ M_\odot\ \text{yr}^{-1}$ (DeCampli 1981; Hartmann, Edwards, and Avrett 1982). Thus, angular momentum loss from such a wind will not be important unless the moment arm provided by the magnetic field is sufficiently large.

While the magnetic field strength and geometries are not predictable from theory or observable (and different mass-loss rate estimates agree to only an order of magnitude), one can present some simple arguments to show that theories for T Tauri mass loss which assume the presence of magnetic fields do not contradict observations of spin-down. The angular momentum loss rate due to wind ejection may be written as (Mestel 1984)

$$-\frac{dJ}{dt} \approx \frac{2}{3}\dot{M}\Omega R^2 \left(\frac{r_A}{R}\right)^n,$$

where $\dot{M}$ is the mass-loss rate, Ω is the angular velocity of the star, r_A is the Alfvén radius, and the exponent n depends upon the assumed magnetic field geometry. The Alfvén radius in this approximation marks the average radial distance to which the magnetic field enforces corotation.

The wind models of Hartmann, Edwards and Avrett (1982), which did not include rotation, assumed for simplicity that the magnetic field lines were purely radial, so that $B(r) \approx r^{-2}$. This suggests application of the simple Weber-Davis (1967) model for spin-down, which assumes a split monopole field configuration. Inserting wind parameters and magnetic field strengths from the Hartmann *et al.* models, and setting $n = 2$ in the above angular momentum loss equation, one predicts braking time scales that are far shorter than indicated by observations.

However, as discussed by Mestel (1968), Rowse and Roxburgh (1981), and Roxburgh (1983), adoption of more realistic field geometries substantially decreases the efficiency of magnetic braking. Using the approximations of Rowse and Roxburgh for a dipolar magnetic field ($n = 1$), the same initial magnetic field strengths and mass-loss rates assumed by Hartmann *et al.* (1982) indicate braking time scales of $\sim 10^6$ yr, in adequate agreement with observations. Thus the requirement that T Tauri stars spin up during pre–main-sequence contraction poses no insuperable difficulties for present theories of mass loss.

c) Emission Activity and Rotation

Main-sequence stars show a well-defined relation between rotation and Ca II or Mg II chromospheric emission (see Noyes *et al.* 1984; Hartmann *et al.* 1984). If dynamo action is responsible for the emission activity of T Tauri stars, one might expect to see a similar correlation in our program stars. Unfortunately, Ca II and Mg II emission fluxes have been reported for very few T Tauri stars (Calvet, Basri, and Kuhi 1984; Calvet *et al.* 1985; Brown, Ferraz, and Jordan 1984), and most of those are high-mass stars. An alternative, well-observed chromospheric diagnostic is Hα emission. Hα is correlated with other

measures of stellar activity in main-sequence stars (Herbig 1985), although interpretations of the data are complicated by the effects of the background photospheric radiation field (Dumont *et al.* 1973; Fosbury 1974; Cram and Mullan 1979). Cohen and Kuhi (1979) showed that Hα emission is correlated with other emission lines in T Tauri stars such as He I and Fe II.

Vogel and Kuhi (1981) found that rapid rotation is more common among non-Hα emission stars. However, this result is suspect because they grouped together stars of very different spectral types. One expects the Hα emission produced by a chromospheric layer to decrease with increasing stellar effective temperature (see Fosbury 1974; Cram and Mullan 1979). Most of the rapid rotators among T Tauri stars are the higher mass objects, which are also the hottest stars. Thus, one would expect to observe a correlation in the sense found by Vogel and Kuhi from radiative transfer effects alone, in the absence of any dependence of chromospheric activity on rotation.

Because we have many more rotational velocity determinations for low-mass stars, we can investigate the relationship between Hα emission and rotation in much narrower ranges of effective temperature, avoiding complications in Hα formation from differing photospheric radiation fields. As shown in Figure 13, we find no correlation between the Hα equivalent widths measured by Cohen and Kuhi (1979) and rotational velocity. Similarly, we find no clear emission-rotation relation for stars between M1 and M4.

Most T Tauri stars have much stronger emission activity than main-sequence stars. One might suppose that Hα emission should decay with increasing age, regardless of rotation. However, we are unable to find any correlation between Hα and luminosity for the same mass stars (Fig. 14).

It may be that errors in placing T Tauri stars in the H-R diagram due to extinction, dust emission, excess line and continuum emission, and time variability are sufficient to mask the underlying correlations between chromospheric activity and rotation and/or age. Or it may be that the use of Hα as a chromospheric diagnostic is complicated by its dependence on wind properties (Hartmann, Edwards, and Avrett 1982). We think it is more likely that emission from T Tauri stars does not depend on the same parameters as solar-type dynamo activity. Emission-line fluxes for T Tauri stars are far above main-sequence levels; plots of chromospheric emission versus age for low-mass stars suggest an abrupt drop in activity from T Tauri levels to main-sequence values (Simon, Herbig, and Boesgaard 1985). Perhaps the mechanism producing the strong emission is different in some way from the magnetic dynamo activity responsible for main-sequence chromospheric emission.

VI. CONCLUSIONS

Most T Tauri stars rotate at rates an order of magnitude or more below breakup velocity, with high-mass stars exhibiting larger rotational velocities than low-mass stars. Large amounts of angular momentum are lost within the first $\sim 10^5$ yr after the end of protostellar accretion, while low-mass T Tauri stars lose at most about three-fourths of their angular momentum during their visible pre–main-sequence contraction. There is evidence that the rotational velocity distribution for T Tauri stars with a common radius is peaked at low rotation values, and has a high-velocity tail.

We have been unable to find a correlation between Hα activity and rotation among low-mass T Tauri stars. Ca II H and K observations of these stars should be examined in light of our rotation data.

Photometric determinations of rotational periods such as those of Rydgren and Vrba (1983), Rydgren *et al.* (1984), and Vrba *et al.* (1985) should be pursued. Used in conjunction with $v \sin i$ data, statistical tests can be made to check the accuracy

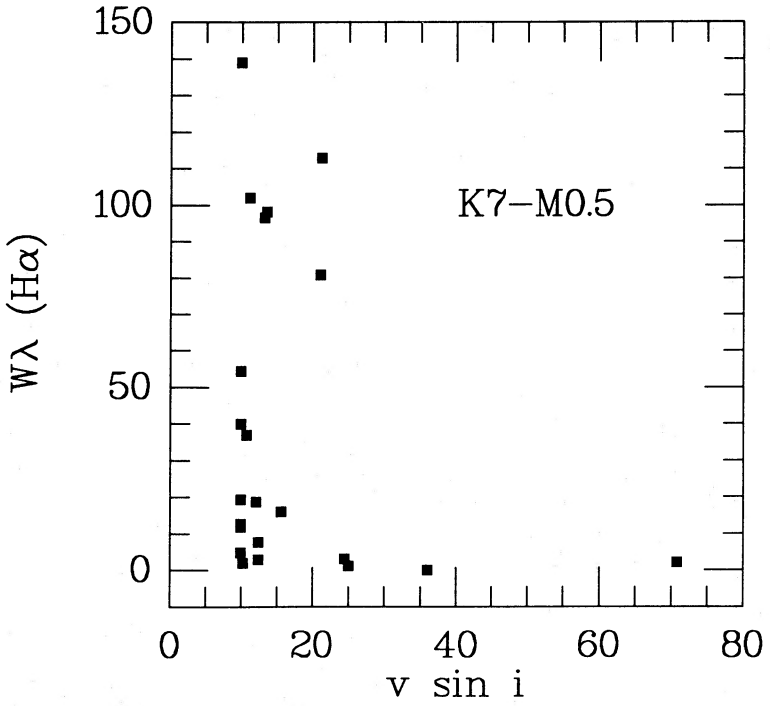

FIG. 13.—Scatter plot of $v \sin i$ vs. Hα equivalent widths from Cohen and Kuhi (1979) for K7–M0.5 stars in our sample

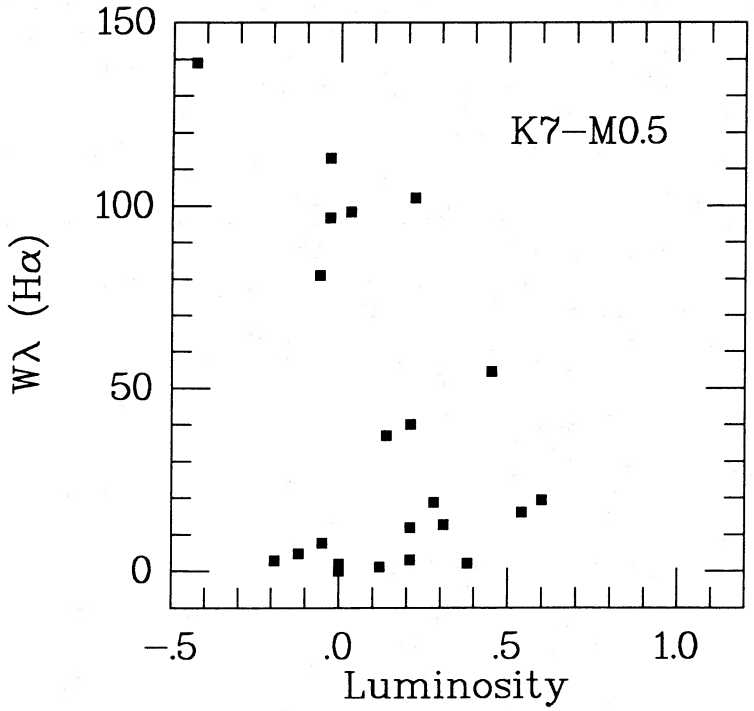

FIG. 14.—Scatter plot of Hα equivalent width vs. stellar luminosity for K7–M0.5 stars above our magnitude limit in Cohen and Kuhi (1979)

of radii for T Tauri stars, and thus investigate the certainty with which T Tauri stars can be placed in the H-R diagram.

We wish to acknowledge useful conversations with M. Geller, A. E. Rydgren, J. Stauffer, S. Strom, and F. Vrba, and we thank R. Gilliland for providing some unpublished calculations of stellar moments of inertia. We also acknowledge the efforts of Jim Peters and Ed Horine in obtaining many of the spectra analyzed in this paper. This work was supported in part by the Scholarly Studies Program of the Smithsonian Institution.

REFERENCES

Abt, H. A., and Hunter, J. 1962, *Ap. J.*, **136**, 381.
Avni, Y., Soltan, A., Tananbaum, H., and Zamorani, G. 1980, *Ap. J.*, **238**, 800.
Bodenheimer, P. 1978, *Ap. J.*, **224**, 488.
Bouvier, D., and Bertout, C. 1986, in preparation.
Brandt, J. C., Wolff, C., and Cassinelli, J. P. 1969, *Ap. J.*, **156**, 1117.
Brault, J. W., and White, O. R. 1971, *Astr. Ap.*, **13**, 169.
Brown, A., Ferraz, M., and Jordan, C. 1984, *M.N.R.A.S.*, **207**, 831.
Calvet, N., Basri, G., Imhoff, C. L., and Giampapa, M. S. 1985, *Ap. J.*, **293**, 575.
Calvet, N., Basri, G., and Kuhi, L. V. 1984, *Ap. J.*, **277**, 725.
Cohen, M., and Kuhi, L. V. 1979, *Ap. J. Suppl.*, **41**, 743.
Cram, L. E. 1979, *Ap. J.*, **234**, 949.
Cram, L. E., and Mullan, D. J. 1979, *Ap. J.*, **234**, 579.
DeCampli, W. M. 1981, *Ap. J.*, **244**, 124.
Dumont, S., Heidmann, N., Kuhi, L. V., and Thomas, R. N. 1973, *Astr. Ap.*, **29**, 199.
Endal, A. S., and Sofia, S. 1981, *Ap. J.*, **243**, 625.
Feigelson, E. D., and Nelson, P. I. 1985, *Ap. J.*, **293**, 192.
Fosbury, R. A. E. 1974, *M.N.R.A.S.*, **169**, 147.
Gilliland, R. L. 1985, *Ap. J.*, **292**, 522.
Goldsmith, P. F., and Arquilla, R. 1985, in *Protostars and Planets*, Vol. **2**, ed. D. C. Black and M. S. Matthews (Tucson: University of Arizona Press), p. 137.
Gray, D. F. 1976, *The Observation and Analysis of Stellar Photospheres* (New York: Wiley).
Hartmann, L., Baliunas, S. L., Duncan, D. K., and Noyes, R. W. 1984, *Ap. J.*, **279**, 778.
Hartmann, L., Edwards, S., and Avrett, E. H. 1982, *Ap. J.*, **261**, 279.
Hartmann, L., Hewett, R., Stahler, S., and Mathien, R. D. 1986, in preparation.
Herbig, G. H. 1957, *Ap. J.*, **125**, 612.
———. 1970, *Mém. Soc. Roy. Sci. Liège*, Ser. 5, **9**, 13.
———. 1977*a*, *Ap. J.*, **214**, 747.
———. 1977*b*, *Ap. J.*, **217**, 693.
———. 1985, *Ap. J.*, **289**, 269.
Herbig, G. H., and Soderblom, D. R. 1980, *Ap. J.*, **242**, 628.
Imhoff, C. L., and Giampapa, M. S. 1980, *Ap. J.* (*Letters*), **239**, L115.
Jones, B. F., and Herbig, G. H. 1979, *A.J.*, **84**, 1872.
Kraft, R. P. 1967, *Ap. J.*, **150**, 551.
———. 1970, in *Spectroscopic Astrophysics*, ed. G. H. Herbig (Berkeley: University of California Press), p. 385.
Larson, R. B. 1984, *M.N.R.A.S.*, **206**, 197.
Latham, D. W. 1982, in *IAU Colloquium 67, Instrumentation for Astronomy with Large Optical Telescopes*, ed. C. M. Humphries (Dordrecht: Reidel), p. 259.
Latham, D. W. 1985, in *Stellar Radial Velocities*, ed. A. G. D. Philip and D. W. Latham (Schenectedy: Davis), p. 21.
Lawless, J. F. 1982, *Statistical Models and Methods for Lifetime Data* (New York: Wiley).
Mestel, L. 1968, *M.N.R.A.S.*, **138**, 359.
———. 1984, in *Cool Stars, Stellar Systems, and the Sun*, ed. S. L. Baliunas and L. Hartmann (Heidelberg: Springer-Verlag), p. 49.
Mouschovias, T. Ch. 1977, *Ap. J.*, **211**, 147.
Mundt, R., and Giampapa, M. S. 1982, *Ap. J.*, **256**, 156.
Myers, P. C., and Benson, P. J. 1983, *Ap. J.*, **266**, 309.
Noyes, R. W., Hartmann, L., Baliunas, S. L., Duncan, D. K., and Vaughan, A. H. 1984, *Ap. J.*, **279**, 763.
Ostriker, J. P. 1970, in *Stellar Rotation*, ed. A. Slettebak (New York: Gordon & Breach), p. 147.
Pallavicini, R., Golub, L., Rosner, R., Vaiana, G. S., Ayres, T. R., and Linsky, J. L. 1981, *Ap. J.*, **248**, 279.
Rowse, D. P., and Roxburgh, I. W. 1981, *Solar Phys.*, **74**, 165.
Roxburgh, I. W. 1983, in *IAU Symposium 102, Solar and Stellar Magnetic Fields*, ed. J. O. Stenflo (Dordrecht: Reidel), p. 449.
Rydgren, A. E., and Vrba, F. J. 1983, *Ap. J.*, **267**, 191.
Rydgren, A. E., Vrba, F. J., Chugainov, P. F., and Shakhovskaya, N. I. 1985, *Bull. AAS*, **17**, 556.
Schatzman, E. 1962, *Ann. Ap.*, **25**, 18.
Simon, T., Herbig, G., and Boesgaard, A. M. 1985, *Ap. J.*, **293**, 551.
Skumanich, A. 1972, *Ap. J.*, **171**, 565.
Smith, M. A., Beckers, J. M., and Barden, S. C. 1983, *Ap. J.*, **271**, 237.
Soderblom, D. R., Jones, B. F., and Walker, M. F. 1983, *Ap. J.* (*Letters*), **274**, L37.
Stahler, S. W. 1983, *Ap. J.*, **274**, 822.

Stahler, S. W., Shu, F. H., and Taam, R. E. 1980, *Ap. J.*, **241**, 637.
Stauffer, J. R., and Hartmann, L. 1986, *Ap. J. Suppl.*, **61**, in press.
Stauffer, J. R., Hartmann, L., Burnham, N., and Jones, B. 1985, *Ap. J.*, **289**, 247.
Stauffer, J. R., Hartmann, L., Soderblom, D. R., and Burnham, N. 1984, *Ap. J.*, **280**, 202.
Terebey, S., Shu, F. H., and Cassen, P. 1984, *Ap. J.*, **286**, 529.
Tonry, J. L. 1981, *Ap. J.*, **246**, 666.
Tonry, J. L., and Davis, M. 1979, *A.J.*, **84**, 1511.
Ungerechts, H., and Thaddeus, P. 1986, preprint.
van Leeuwen, F., and Alphenaar, P. 1982, *ESO Messenger*, No. 28, p. 15.
Vogel, S. N., and Kuhi, L. V. 1981, *Ap. J.*, **245**, 960.
Vrba, F. J., Rydgren, A. E., Zak, D. S., Chugainov, P. F., and Shakhovskaya, N. I. 1984, *Bull. AAS*, **16**, 998.
Walter, F. M. 1982, *Ap. J.*, **253**, 745.
Weber, E. J., and Davis, L., Jr. 1967, *Ap. J.*, **148**, 217.

Note added in proof.—D. Bouvier, C. Bertout, A. O. Benz, and M. Mayor (*Astr. Ap.*, in press) have recently presented rotational velocities derived from a variety of methods for 28 T Tauri stars. There are seven stars with spectroscopic determinations of $v \sin i$ in common with our survey; the agreement is good. Bouvier *et al.* find a distribution of rotational velocities for low-mass stars that is quite similar to ours.

L. Hartmann, R. Hewett, and R. D. Mathieu: Center for Astrophysics, 60 Garden St., Cambridge, MA 02138

S. W. Stahler: Department of Physics, MIT, Cambridge, MA 02139